No. F.R.Note No. 472
Research Programme
Objective D.11

DEPARTMENT OF SCIENTIFIC AND INDUSTRIAL RESEARCH AND FIRE OFFICES' COMMITTEE
JOINT FIRE RESEARCH ORGANIZATION

THE FLOW RESISTANCE OF SOME FLAME ARRESTER ELEMENTS

by

P. G. Quinton

Summary

A survey has been made of published data on the flow resistance of the types of porous structure commonly incorporated into flame arresters. These structures have included gauzes, crimped ribbon matrices, perforated plates, and packed beds of loose and consolidated granular materials.

No single correlation relating pressure drop and flow rate to the properties of the porous material and the flowing gas could be applied to all types of porous material. However, the flow resistance of gauzes and beds of spheres could be expressed in a single equation over a limited range of Reynold's numbers. Data for crimped ribbon matrices were similar to those expected from flow in a uniform tube, with allowance made for entry and exit pressure losses, and for the undeveloped flow in some of the length. In the case of perforated plates, the main pressure loss occurred at entry and exit, with a minor loss due to friction in the passage. Nomograms are presented for the ready solution of the resulting equations, with some examples of their use and comparison of predicted values with experimental results. The ranges of flow rates, pressure drops and aperture sizes covered in the nomograms are such as would be common in industrial plant working under normal conditions.

"Full-scale copies of figures 5,6,7,8 may be obtained on application to the Joint Fire Research Organization".

April 1961

F.1000/10/84B

Fire Research Station
Boreham Wood,
Herts.

THE FLOW RESISTANCE OF SOME FLAME ARRESTER ELEMENTS

by

P. G. Quinton

INTRODUCTION

Various types of flame arrester are in use to prevent the continued propagation of gas and vapour explosions in industrial plant. They are installed in ducts carrying solvent vapour, in the delivery pipeline to appliances using premixed combustible gases, and in many other systems in which the explosion risk is present. The selection of an efficient flame arrester from amongst the various types depends both on its operating pressure drop and on its ability to quench flame. Work (1) which has been done on the latter property has led to the following generalizations:-

(1) the effective arrester aperture dimension varies inversely with the incident flame speed, provided that the dimension is less than the quenching diameter.

(2) the effective depth varies directly with the incident flame speed.

It follows from Reynolds analogy between heat and momentum transfer that a high flow resistance also implies a high heat transfer coefficient. Therefore, the more effective flame arrester of a given type has the higher pressure drop, for a given gas velocity. The purpose of the present note is to bring together pressure loss data on the various types of flame arrester and to select for each the most suitable method of correlation. The correlations apply to flame arresters installed in plant operating under ordinary conditions, in the absence of any explosion or fire, and calculations based on the correlations are for air at atmospheric temperature and pressure.

Flame arresters were found to fall into four classes for the purpose of correlation of their flow resistance:

(1) loose or consolidated granular beds,

(2) single or packed gauzes,

(3) flame arresters with uniform apertures and high depth/diameter ratios, and

(4) flame arresters with uniform apertures and low depth/diameter ratios.

Class 3 includes crimped ribbon matrices, flat plates stacked parallel to the direction of flow, and perforated blocks; whilst class 4 consists of perforated plates. Only a few (2,3,4,5) researches on flame arresters have included data on flow resistance. However, there has been considerable study of the flow resistance of porous materials in general, with particular emphasis on granular beds and gauzes.

SURVEY OF METHODS OF CORRELATION

Two dimensionless groups, a resistance coefficient and a Reynolds number, are needed for the correlation of data on flow through porous materials. The general resistance coefficient, N_{cr}, may be defined as:-

$$N_{cr} = \frac{R}{\rho U^2} \qquad (1)$$

where R = fluid shear stress at a solid boundary

ρ = fluid density

U = velocity of fluid approaching arrester

and the Reynolds number, N_{Re}, as:-

$$N_{Re} = \frac{\rho U d}{\mu} \qquad (2)$$

where d = characteristic aperture dimension

μ = fluid viscosity

Several expressions have been proposed for N_{cr} and N_{Re} depending upon the type of material under consideration, upon the definition chosen for d, and upon the porosity of the material. It was found necessary to divide porous materials into two broad classes for the purpose of correlating resistance coefficient with Reynolds number. On the one hand were those with irregular passages such as gauzes and granular beds, and on the other hand those with uniform passages, for example, crimped ribbon matrices and perforated plates. The behaviour of the two groups of porous materials will now be considered in turn. The equations used in the different treatments of flow through porous materials are given in Table 1.

Non - uniform apertures

The Kozeny - Carman model

The model was that of a bundle of capillaries with their axes parallel to the direction of flow, and was originally applied to granular beds. An account of the model may be found in Ref (6). The hydraulic diameter, d', was defined as the volume of channels per unit surface area of solid. If S is the specific surface of the solid, i.e. surface per unit volume of the particle, then $d' = \frac{e}{(1-e)S} = \frac{ed}{6(1-e)}$ for spheres

where e = volumetric porosity

d = diameter of particle, or equivalent spherical diameter.

The velocity used was the mean channel velocity, V.

$$V = \frac{U}{e}$$

The expression for R results from a force balance over the bed:

$$R = \frac{he}{L(1-e)S}$$

Thus, the two groups defined in equations 1 and 2 become

$$N_{cr} = \frac{he^3}{LS(1-e)\rho U^2}$$

$$N_{Re} = \frac{\rho U}{S\mu(1-e)}$$

It was found experimentally that at low Reynolds numbers

$$N_{cr} \cdot N_{Re} = K'' \qquad (3)$$

where K" is the Kozeny - Carman constant. The constant has a value of about 5 at 40% volumetric porosity, and varies with the porosity, shape, and orientation of the particles (7).

At higher Reynolds numbers equation 3 requires modification. An expression given by Carman (8) for values of Reynolds numbers up to 1000 was

$$N_{cr} = \frac{5}{N_{Re}} + \frac{0.4}{N_{Re}^{0.1}} \qquad (4)$$

Equation 4 has been used to correlate N_{cr} and N_{Re}, and is shown in Table 1 and in Fig 1 (Curve A).

The expressions for N_{cr} and N_{Re} in Table 1 may be used for both beds of spheres and packs of gauzes, if, in the latter case, the bed depth is defined as the product of twice the wire diameter and the number of gauzes in the pack.

The Rose Correlation

The method of correlation used by Rose (9) differed from the Kozeny - Carman treatment in the definitions of characteristic aperture dimension and of the functions of porosity used in defining the dimensionless groups. An empirical porosity function was found which would make the correct allowance for the effect of porosity on resistance coefficient. The characteristic aperture dimension which he selected (d) was the diameter of the sphere with the same specific surface as the particles constituting the bed. The resistance coefficient was defined as

$$N_{cr} = \frac{hd}{\rho U^2 L F(e)}$$

where F(e) is an empirical porosity function,

and the Reynolds number was defined as

$$N_{Re} = \frac{U\rho d}{\mu}$$

At low Reynolds numbers (less than 1.0) the relation between these two groups was

$$N_{cr} \cdot N_{Re} = 1000 \qquad (5)$$

At higher values of Reynolds number (up to 1000) the relation for smooth spheres was

$$N_{cr} = \frac{1000}{N_{Re}} + \frac{125}{N_{Re}^{0.5}} + 14 \qquad (6)$$

This correlation is given in Table 1.

The Rose porosity function was empirical, and was approximately equal to $\frac{2.4\,(1-e)^{3.5}}{e}$, whereas that derived from the Kozeny - Carman equation (equation 3) was equal to $\frac{0.18(1-e)^2}{e^3}$. The relationship between the two porosity functions is shown in Fig.2, and over the porosity range 0.33 to 0.8 the functions do not differ from each other by more than 20 per cent. Fig.2 is only valid in the range of Reynolds numbers for which equations 3 and 5 apply.

The Grootenhuis Correlation

Much of the published data on the flow resistance of gauzes has been correlated by Grootenhuis (10). The definition of Reynolds number was based on the actual velocity in the passages, and a hydraulic diameter was defined as the volume of channels per unit surface area. The expression for hydraulic diameter differed from that used by Kozeny or Carman in that the volume of channels was based on the throat, or minimum area, of an aperture. Grootenhuis' expressions for the resistance coefficient and for the Reynolds number were

$$N_{cr} = \frac{hde^2}{4t(1-e)\rho U^2}$$

$$N_{Re} = \frac{\rho Ud\,(1-Md)^2}{4\mu e(1-e)}$$

where d = wire diameter
t = thickness of gauze or pack of gauzes
M = meshes/unit width

The correlation between N_{cr} and N_{Re}, given by Grootenhuis, was

$$\log 15\, N_{cr} = 1.75\, N_{Re}^{-0.203} \qquad (7)$$

and this equation is listed in Table 1.

It may readily be shown that the resistance coefficients and Reynolds numbers defined by Grootenhuis and by Kozeny are related as follows:

$$\frac{N_{cr}\ (\text{Kozeny})}{N_{cr}\ (\text{Grootenhuis})} = e$$

$$\frac{N_{Re}\ (\text{Kozeny})}{N_{Re}\ (\text{Grootenhuis})} = \frac{e}{(1-Md)^2}$$

Mean values of e and $e/(1-Md)^2$ for the gauzes studied by Grootenhuis were 0.699 and 1.52 respectively. Using these values, equation 7 can be adjusted so that the resistance coefficient and the Reynolds number are identical to those of Kozeny. The equation then becomes

$$\log 21.4\, N_{cr} = 1.90\, N_{Re}^{-0.203} \qquad (8)$$

where N_{cr} and N_{Re} are as defined by Kozeny.

Equation 8 is plotted in Fig 1 (Curve B) alongside the corresponding curve for smooth spheres based on the Kozeny - Carman correlation (Curve A). The values of the resistance coefficient agree to within about 25 per cent, over the range of Reynolds numbers 1 to 1000.

Other methods of correlation

Some workers [11] have related the flow resistance of a porous material to the friction chart for a smooth pipe by means of factors dependent on the porosity of the material and the shape of the particles. The method has been extended to consolidated porous media by the use of an effective porosity. This effective porosity was lower than the total porosity.

Another approach was used by Green and Duwez [12] in their work on sintered metals. They showed that the pressure drop through a bed could be equated to the sum of viscous and inertial losses by an equation of the form:

$$\frac{h}{L} = AV + BV^2 \qquad (9)$$

where A and B depended on particle geometry and bed porosity. In general, the relationship between A or B and porosity would need to be determined experimentally.

Uniform apertures

The flow through a flame arrester consisting of a number of similar uniform passages has been treated in the same way as the case of flow in a uniform pipe [2] [3]. The resulting expressions depended on the depth/diameter ratio of the arrester channel, and published work on flow resistance of crimped ribbon flame arresters has dealt only with the case of high depth/diameter, or aspect, ratio.

Class I - Large aspect ratio

The pressure loss resulting from passage of fluid through such an element may be divided into two parts;

(1) that resulting from acceleration of fluid at entry to the apertures, and retardation at exit, with consequent turbulence, and

(2) the normal pipe friction losses.

Lindley [3] showed that an expression for the sum of entrance and exit losses (z) may be calculated from the porosity of the arrester element. The value of z was subtracted from the overall resistance coefficient and the difference plotted against the Reynolds number in the aperture. With streamline flow, the channels with the lower aspect ratios had relatively higher frictional resistance coefficients for a given Reynolds number.

Lindley concluded that with streamline flow in the aperture but turbulent flow in the duct:-

$$N_{cr} = K N_{Re}^{n} \qquad (10)$$

An examination of his results showed that over a range of aspect ratios 30 to 120 the aspect ratio appeared to be significant. It was therefore postulated that

$$N_{cr} = K N_{Re}^{n} \left(\frac{L}{d}\right)^{w} \qquad (11)$$

A multiple regression analysis was made of Lindley's results up to aspect ratios of 120 and Reynolds numbers of 2000 to find the best values of K, n and w. The resulting equation , with a correlation coefficient of 90% is given below.

$$N_{cr} = 5.15 \; N_{Re}^{(-0.918 \pm x)} \left(\frac{L}{60d}\right)^{(-0.335 \pm y)} \qquad (12)$$

The values of x and y in the above equation define the 95% confidence limits ($x = 0.030$ and $y = 0.070$). This equation has been plotted in Fig.4. and includes some of the points obtained by Lindley. The results of Cubbage (2) working with crimped ribbon matrices, Kreith and Eisenstadt (13) working with single short tubes, and Loisin, Chainaux and Delclaux (5) who investigated parallel stacked plates agreed fairly closely with equation 12.

Cubbages results were close to the Poiseuille equation, viz,

$$N_{cr} = \frac{8}{N_{Re}} \qquad (13)$$

but with resistance coefficients 13% lower than would be expected from this equation. A possible explanation for this depends on the state of flow upstream of the arrester. In Cubbage's experiments, unlike Lindley's, the flow in the duct leading to the arrester was not always fully turbulent and thus there would be less energy lost in the transition to streamline flow in the apertures. In practice the flow in industrial ducting would be turbulent and equation 12 more likely to apply than the Poiseuille equation.

For practical purposes, equation 12 can be rearranged:

$$h = 1.14 \times 10^{-4} \left(\frac{U}{e}\right)^{1.082} \frac{L^{0.665}}{d^{1.583}} \quad \text{inches water gauge} \qquad (14)$$

when the fluid is air at N.T.P., and the aspect ratio is 15 to 150 and Re $<$ 2000 (V in f.p.s)

For aspect ratios above 150, and Re less than 2000 there is evidence that aspect ratio is no longer significant, and it is suggested that Lindley's equation provides a better correlation than equation 12, viz:

$$N_{cr} = \frac{4.0}{N_{Re}^{0.9}} \qquad (15)$$

Above a value of $N_{Re} = 2000$ in the apertures the flow is turbulent and the flow is best represented by an equation due to Lindley in which the aspect ratio does not influence the resistance coefficient for a given Reynolds number. The equation appears in Table 1.

Glass II - Small aspect ratio

The pressure loss resulting from flow through a relatively short aperture, of aspect ratio less than 5, may be regarded as being mainly due to inlet and exit losses, and therefore should not be so dependent on the depth and diameter of the apertures.

With aspect ratios below about 5 it is necessary to calculate the pressure drop from charts relating orifice coefficient to Reynolds number, aspect ratio and porosity. An arrester with an aspect ratio of 5 usually takes the practical form of a perforated plate or block. The following equation for the pressure drop across a perforated plate has been derived from the results of Kolodzie (14) et al.and Smith et al.(15).

$$h = 2.2 \times 10^{-4} \; V^2 \left(\frac{0.905}{e}\right)^{0.10} (1 - e^2) \; K \text{ in.water} \qquad (16)$$

where V in f.p.s. is the aperture velocity, and $K = 1/C_d^2$

SUITABLE EXPRESSIONS FOR FLOW THROUGH FLAME ARRESTER ELEMENTS

Elements with non-uniform apertures

The results for sintered metals, beds of spheres, and wire gauzes were expressed in terms of the Kozeny - Carman model and are shown in Fig.1. The uppermost line (Curve A) was based on equation 4, suggested by Carman (8) for flow through granular beds. Curve B was based on Grootenhuis' results for wire gauzes (10), as expressed by equation 8. Curve C is the best line through some values for sintered metals, given by Grootenhuis (16). Over a range of Reynolds numbers from 3 to 100 the agreement between the results for gauzes and granular beds was satisfactory, but the divergence outside this range makes it necessary to consider the two types separately.

Sintered metals and beds of spheres

In the light of work by Coulson (7) on the effect of porosity on flow resistance, the Rose equation was selected for correlating the flow resistance of beds of spheres in preference to the Carman equation. In addition the results on the flow resistance of sintered metals (16) were found to correlate better by use of the Rose equation than the others (8,11) which have been discussed. A nomogram (Fig.6) for solving the Rose equation has been given in the appendix.

Gauzes

Some data (17,18,19), which have been published since Grootenhuis' work (10), have been compared in Fig.3 with the original Grootenhuis curve expressing the flow resistance of gauzes. The agreement appears satisfactory. As a result of the observation (20) that mesh size and wire diameter of commercial wire gauzes were related, the Grootenhuis equation could be reduced to three variables for a given gas mixture. These variables are gas velocity, pressure drop per gauze and mesh size. An alignment chart for the pressure drop across gauzes has been given in the appendix (Fig.5).

Elements with uniform apertures

Arresters with a high aspect ratio

In the case of flame arrester elements of high aspect ratio the method of correlation given by Lindley (3) was closely followed. The algebraic expressions employed have been given in Table 1. A nomogram, based on equation 14, is given in Fig.7 and it should be applicable over the range of aspect ratios 15 to 150. From the nomogram the pressure drop across crimped ribbon arresters may be read off.

Arresters with a low aspect ratio

The pressure drop across thin arresters of low aspect ratio, is mainly due to inlet and exit losses. A nomogram, based on equation 16, is shown in Fig.8 and from it may be determined the pressure drop across perforated plate arresters.

CONCLUSIONS

It has been found that porous materials used in flame arrester elements may be divided into two main classes when considering their flow resistance. First, there are beds of spheres and wire gauzes which can be approximately related to the common property of specific surface. The other class consisted of elements having straight, uniform, flow passages.

Materials having straight uniform passages were further subdivided on the basis of the aspect ratio. When the latter is large the flow is similar to that expected in a number of uniform pipes in parallel with allowance made for entry length. Below an aspect ratio of 5, the flow resistance is defined in terms of an orifice coefficient, which shows a complex variation with the passage Reynolds number and aspect ratio.

Nomograms for calculating the resistance of arresters of various types, and appropriate instructions for their use are given.

SYMBOLS

A, B	-	constants
C_d	-	a discharge coefficient (Table 1)
d,	-	characteristic linear dimension
d', de	-	hydraulic diameter of aperture
e	-	volumetric porosity = $\frac{\text{volume of free space}}{\text{total volume}}$
$F(e)$	-	the Rose function of porosity
h	-	pressure drop across porous material
H_e	-	crimp height including metal thickness
K	-	$1/C_d^2$
K''	-	Kozeny - Carman constant.
L	-	depth of an arrester element
$\frac{L}{d}$	-	$\frac{\text{depth}}{\text{diameter}}$ or aspect ratio
m	-	shortest distance between adjacent wires in a wire gauze
M	-	number of meshes/ unit width
μ	-	viscosity of fluid
n	-	a constant
N	-	number of gauzes in an arrester element
N_{cr}	-	resistance coefficient
N_{Re}	-	Reynolds number
ρ	-	density of fluid
R	-	shear stress at solid boundary
S	-	specific surface of a material
t	-	thickness of a pack of gauzes, or of metal in a crimped ribbon
U	-	the approach velocity to an arrester
V	-	the aperture velocity in an arrester element
w	-	a constant
x	-	standard deviation of n
y	-	standard deviation of w
z	-	the sum of entry and exit pressure losses. $= \frac{d}{8L}(1.5 - e)^2 + (1 - e)^2$
θ	-	crimp angle

REFERENCES

(1) Palmer,K.N. and Tonkin,P.S. F.R.Note No.438 1960

(2) Cubbage,P.A. Gas Council Research Communication G-C 63, 1959

(3) Lindley,B.C. J.R.Aero.Soc., 1959 63 597-602

(4) Egerton,A., Everett,A.J. and Moore,N.P.W. 4th Symposium on Combustion pp.689 - 695.

(5) Loisin,R., Chainaux,L., and Delclaux,J. Paper 37, 8th Int. Conference Directors of Safety in Mines 1954.

(6) Coulson,J.M., and Richardson,J.F. "Chemical Engineering" Vol. II. Pergamon Press. London 1954.

(7) Coulson,J.M. Trans.Inst.Chem.Eng. 1949 27 237-257

(8) Carman,P.C. Trans.Inst.Chem.Eng., 1937 15 150

(9) Rose,H.E. Proc.Inst.Mech.Eng., 1945 135 148-153

(10) Grootenhuis,P. Proc.Inst.Mech.Eng. 1954 168 (34) 837 - 46

(11) Brownell,L.E., Gami,D.C., Miller,R.A., and Nekarvis,W.F. J.Amer. Inst.Chem.Eng. 1956 2 79

(12) Green,L., and Duwez,P. Trans.Amer.Soc.Mech.Engrs. 1951 73 39 - 45

(13) Kreith,F., and Eisenstadt,R. Trans.Amer.Soc.Mech.Engrs. 1957 79 1070-8

(14) Kolodzie,P.A., and Van Winkle,M. Amer.Inst.Chem.Eng. 1957 Vol.3 303 - 312.

(15) Smith,P.L., and Van Winkle,M. J.Amer.Inst.Chem.Eng., 1958 4 266-8

(16) Grootenhuis,P. Engineering 1949, 167 (4340),291-2

(17) Townsend,A.A. Quarterly J. Mech. and Applied Maths. 1951, 4 (3) 308 - 320

(18) Tong, L.S. Dept.Mech.Eng., Stanford University, Stanford, California. Tech. Report 28 April 1956

(19) Coppage,J.E., London,A.L. Chem.Eng.Progr. 1956 52 (2) 57F-63F

(20) Palmer, K.N. 7th Symposium on Combustion pp. 497-503

TABLE 1

Equations for the Flow Resistance of Porous Materials

Investigator	Application	Range of variables.	N_{cr}	N_{Re}	Correlation
Carman	Packed beds: may be extended to single and packed gauzes	$N_{Re} < 1000$	$\frac{he^3}{LS\rho U^2(1-e)}$	$\frac{U\rho}{S\mu(1-e)}$	$N_{cr} = \frac{5}{N_{Re}} + \frac{0.4}{N_{Re}^{0.1}}$
Rose	Packed beds: applies to nearly spherical particles	$3 < N_{Re} < 1000$	$\frac{hd}{L\rho U^2 F(e)}$	$\frac{U\rho d}{\mu}$	$N_{cr} = \frac{1000}{N_{Re}} + \frac{125}{N_{Re}^{0.5}} + 14$
Grootenhuis	Single and packed gauzes	$N_{Re} < 5000$	$\frac{hde^2}{4t(1-e)\rho U^2}$	$\frac{\rho Ud(1-Md)^2}{4\mu e(1-e)}$	$\text{Log } 15N_{cr} = 1.75\ N_{Re}^{-0.203}$
Lindley	Crimped ribbon materials	$N_{Re} < 2000$ $N_{Re} > 2000$	$\frac{hde^2}{4\rho U^2 L} - z$	$\frac{U\rho d}{\mu e}$	$N_{cr} = \frac{4.0}{N_{Re}^{0.9}}$ $N_{cr} = \frac{0.353}{N_{Re}^{0.58}}$
This note	Modified Lindley equation for high aspect ratio	$\frac{L}{d}$: 15 - 150 $N_{Re} < 2000$ $N_{Re} > 2000$	$\frac{hde^2}{4\rho U^2 L} - z$	$\frac{U\rho d}{\mu e}$	$N_{cr} = \frac{5.15}{N_{Re}^{0.918}} \left(\frac{60d}{L}\right)^{0.335}$ $N_{cr} = \frac{0.353}{N_{Re}^{0.58}}$
Kolodzie et.al.	Perforated Plates	$N_{Re} < 10000$	$C_d = \frac{U}{e}\left(\frac{1-e^2}{2gh}\right)^{0.5}$	$\frac{U\rho d}{\mu e}$	See Fig. 8

APPENDIX

Description of alignment charts for the solution of pressure loss equations

Wire Gauzes

Fig.5 for wire gauzes contains only three variables, the approach velocity in feet per second, the mesh width, or distance between wires in inches, and the pressure loss per gauze (inches water gauge).

Example:

The pressure drop/gauze for an aperture of 0.02 inch and an approach velocity of 10 f.p.s. is found from fig.5 as 0.086 inch w.g. An equation given by Cubbage [2], p.27, gives a value of 0.13 inch w.g./gauze, allowing each of the two perforated plates which supported the ten gauzes a pressure loss equal to that of one gauze.

Sintered metals and granular beds.

Fig.6 is used as follows. A vertical is taken through the point representing particle diameter, and the join with the appropriate sloping velocity line (U) is projected horizontally on to the axis marked A. From this point on A, a line is drawn to cut the e, or porosity, scale at the desired value. The point at which this line cuts the axis B is joined through the value of $\frac{L}{d}$ to the C axis. The corresponding point on the C axis is joined by a straight line connecting the approach velocity (axis marked U) to the required pressure loss (in.water gauge) on the 'h' scale.

The example, shown as a dotted line, is for a bed of 0.1 inch diameter particles with an approach velocity of 1.f.p.s. The bed porosity is 40 per cent and it is 10 inch or 100 particle diameters in depth. A pressure drop of 2.6 inch w.g. from the chart compares with 2.3 inch w.g. by calculation from the Rose equation (Table 1).

Arresters of large aspect ratio

The solution of equation (14) for crimped ribbon type flame arresters is given graphically in Fig.7. Entrance and exit losses have been neglected, since it was calculated that they represented a negligible proportion of the resistance to flow for normal operating conditions.

The use of the chart is illustrated in the following example on an arrester specified in Ref.3. This arrester, described as No.6 in the above paper, had an aperture hydraulic diameter, d_e, of 0.024 inch a depth of 1.0 inch and a porosity of 82.7 per cent. (Its pressure loss at 20 f.p.s. was given in Fig.2 of Ref.3 as 1.7 inch w.g.). The pressure loss from the chart, Fig.7, is found by drawing a line from a porosity of 82.7 per cent on the 'e' scale through reference line R_1 to the arrester depth, 1.0 inch on the L scale. The join with R_1 is connected by a straight line through the value of 0.024 inch on the hydraulic diameter or 'd_e' scale to cut the R_2 scale. The line joining the velocity of 20 f.p.s. on the U scale to this point on the R_2 scale cuts the h, or pressure loss scale, at 1.3 inch w.g.

When allowance is made for the considerable scatter in the data on which the nomogram is based, and errors in its construction and use, the agreement between experimental and estimated pressure drop appears reasonable. The agreement between Cubbage's [2] results and the estimate from Fig.7 was generally closer, e.g. (p.29 of the above paper), flame arrester type G has a loss of 1.1 inch w.g. at 10 f.p.s., whereas the chart, Fig.7, leads to a figure of 1.0 inch w.g. at 10 f.p.s.

In practice, there is some difficulty in selecting the hydraulic diameter to be used in the nomogram. If it is assumed that blockage due to material other than the crimp metal is negligible, then the following equations may be used to estimate 'd_e'. The first, Eq.17 is valid for any aperture shape, provided blockage and metal thickness are known.

$$\text{the hydraulic diameter, } d_e = \frac{2et}{1-e} \qquad (17)$$

where e = porosity or fractional free area
t = metal thickness (in.)

The second, (Eq.18), applies to the arrester for which crimp height and blockage are known and for which the apertures may be treated as isosceles triangles. In this case:-

$$d_e = \frac{2H_e}{(1 + \frac{\sec\theta}{e})} \qquad (18)$$

where H_e = crimp height (in)

θ = triangle base angle (usually 45°)

Elements of small aspect ratio

A graphical solution to the flow resistance equation for perforated plates is given in Fig.8. Its use is illustrated by the following example for a perforated plate with a hole diameter, d, of 0.01 inch a depth/diameter ratio, $\frac{L}{d}$, of 4, a hole velocity (V) of 50 f.p.s. and a porosity of 30 per cent. First a line is drawn from the velocity scale marked V through the hole diameter; d; to cut the reference line R_1. This point on R_1 is projected horizontally to cut a vertical projection through the $\frac{L}{d}$ value of 4 to give the appropriate 'K' value (1.85). A line is also drawn linking the velocity on the V axis to the value of porosity and the point at which this line cuts the R_2 axis is joined through K = 1.85 to give the required pressure drop of 1.1 inch w.g. This compares with a value of 1.0 by calculation from equation 16.

Accuracy of the predicted value

It has been estimated that the maximum error likely to result from a systematic alignment error of 0.05 inch, would be of the order of 10 per cent for the nomograms discussed, without allowing for errors in construction.

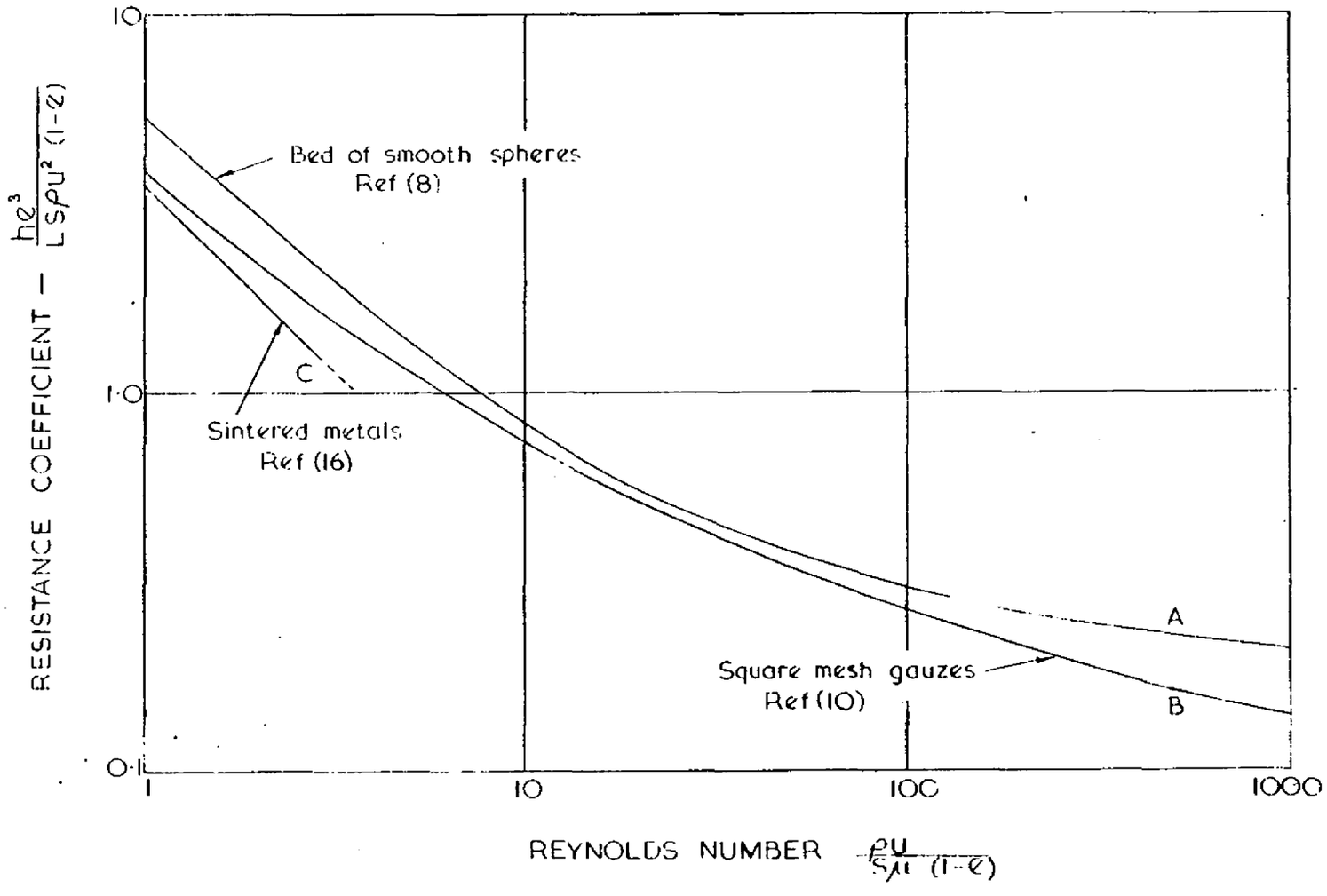

FIG 1 CORRELATION OF RESISTANCE COEFFICIENT WITH REYNOLDS NUMBER

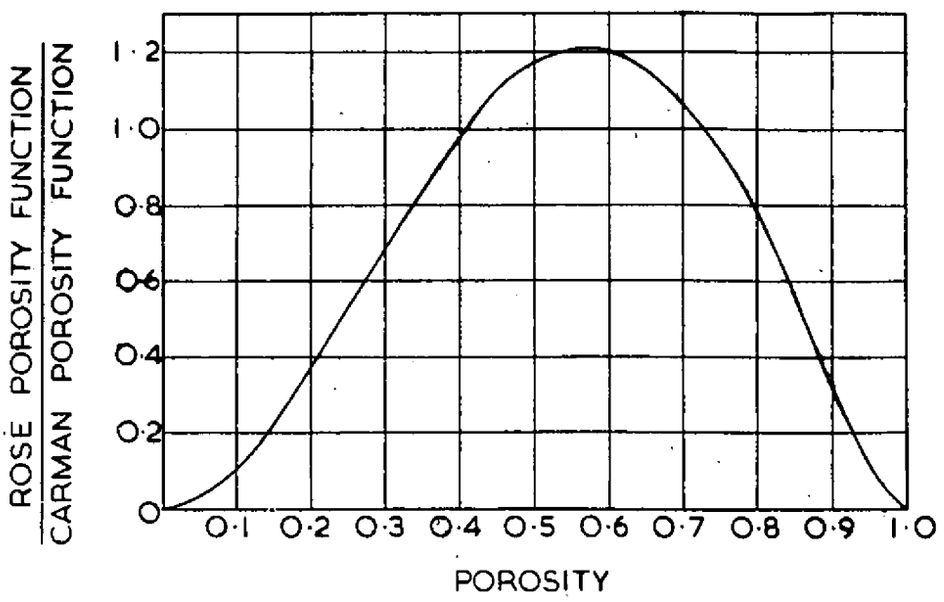

FIG. 2 RELATIONSHIP BETWEEN ROSE AND CARMAN POROSITY FUNCTIONS

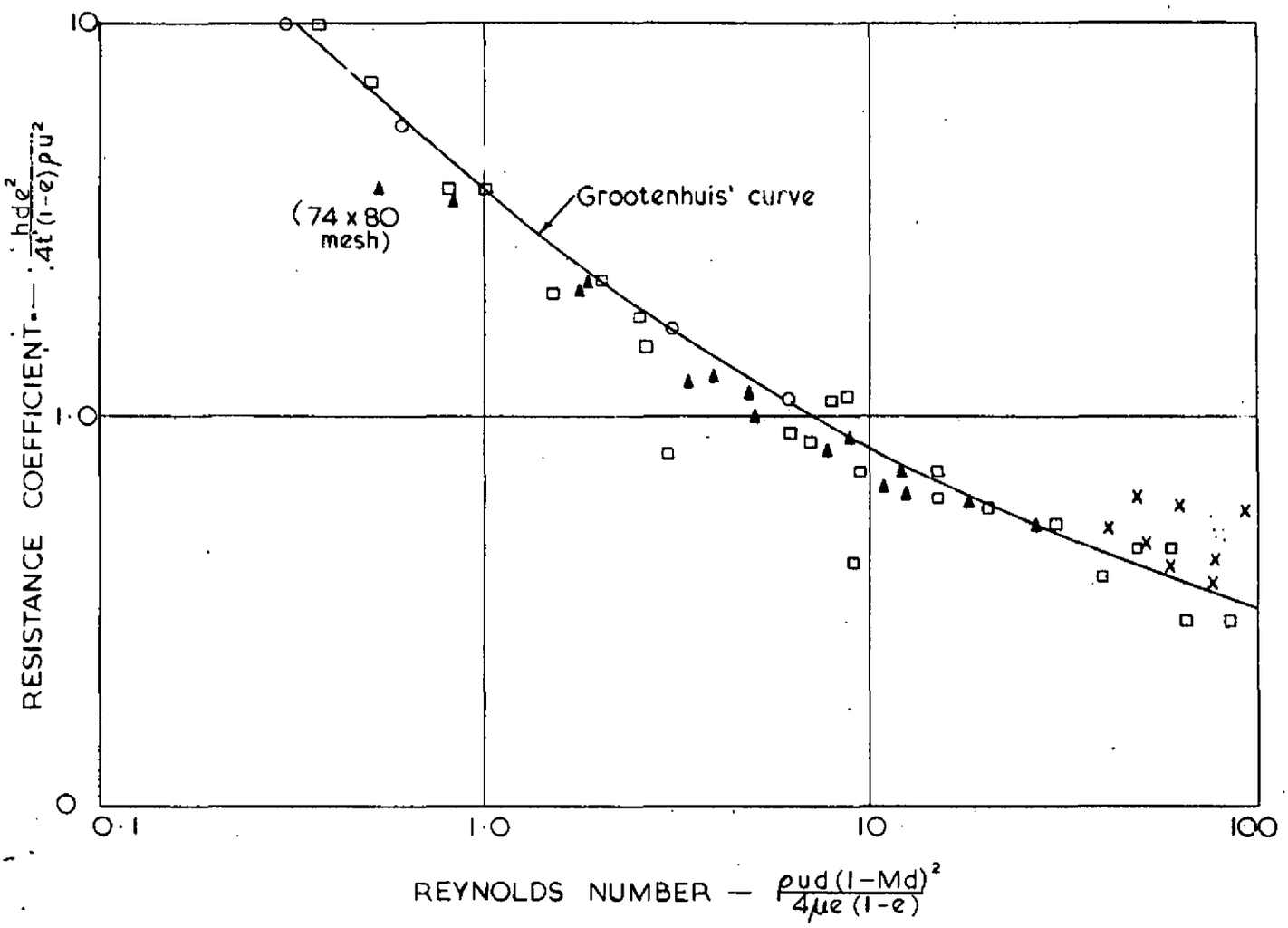

- o Coppage and London (19)
- x Townsend (17)
- ▲ Tong (18)
- □ Grootenhuis (10)

FIG. 3. RESISTANCE TO FLOW OF WIRE GAUZES

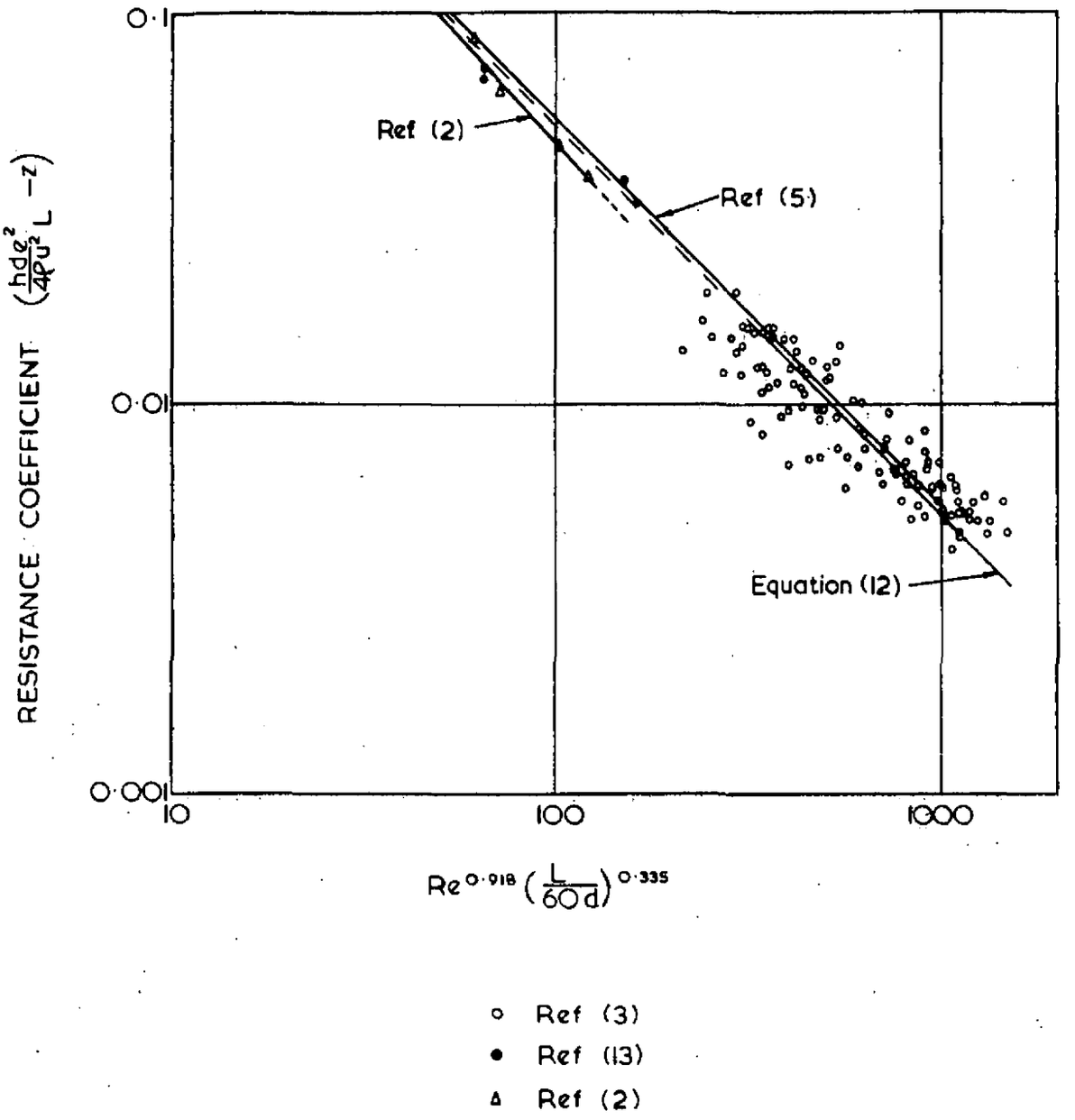

FIG. 4. FLOW RESISTANCE OF UNIFORM CHANNEL MATRICES

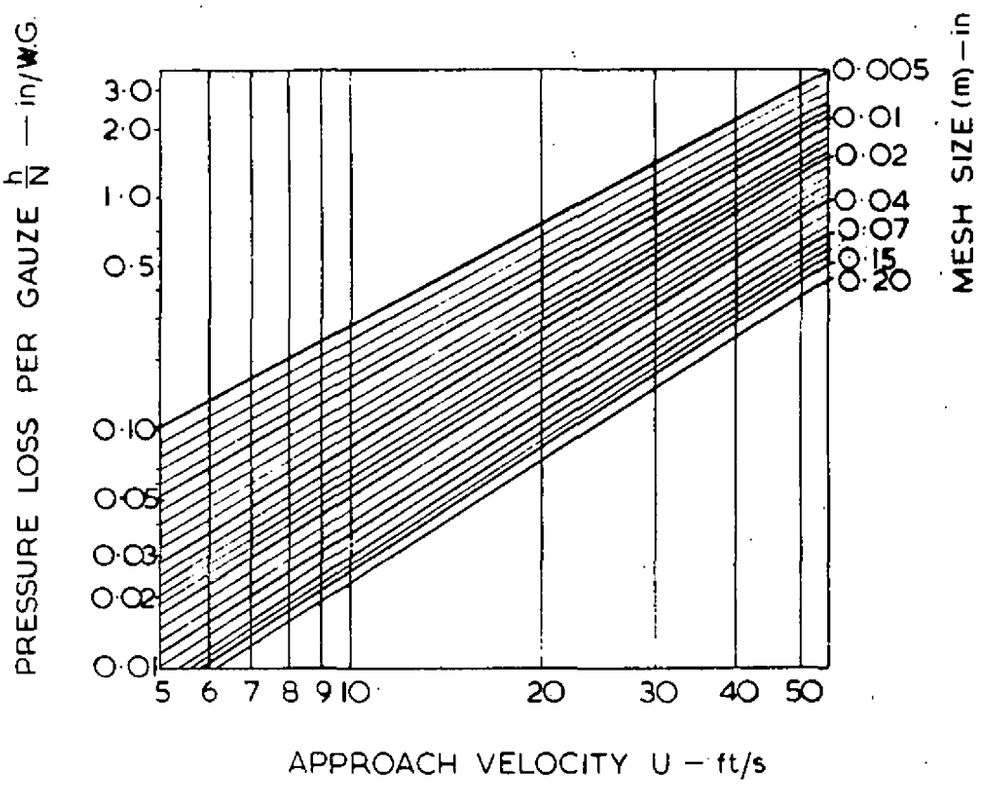

FIG. 5. PRESSURE-DROP CHART FOR WIRE GAUZE FLAME ARRESTERS

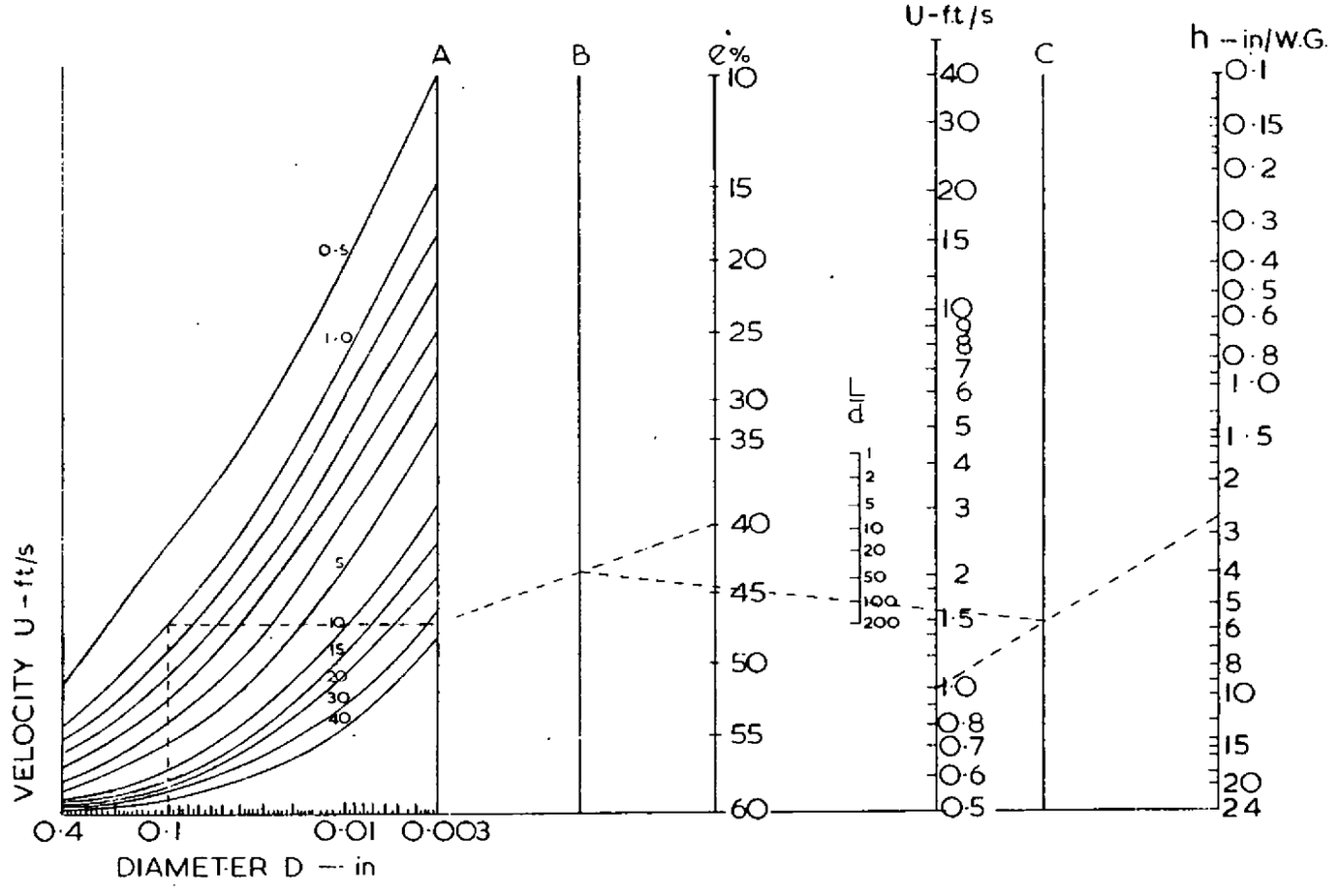

FIG. 6. NOMOGRAM FOR PRESSURE DROP ACROSS PACKED BEDS AND SINTERED METALS

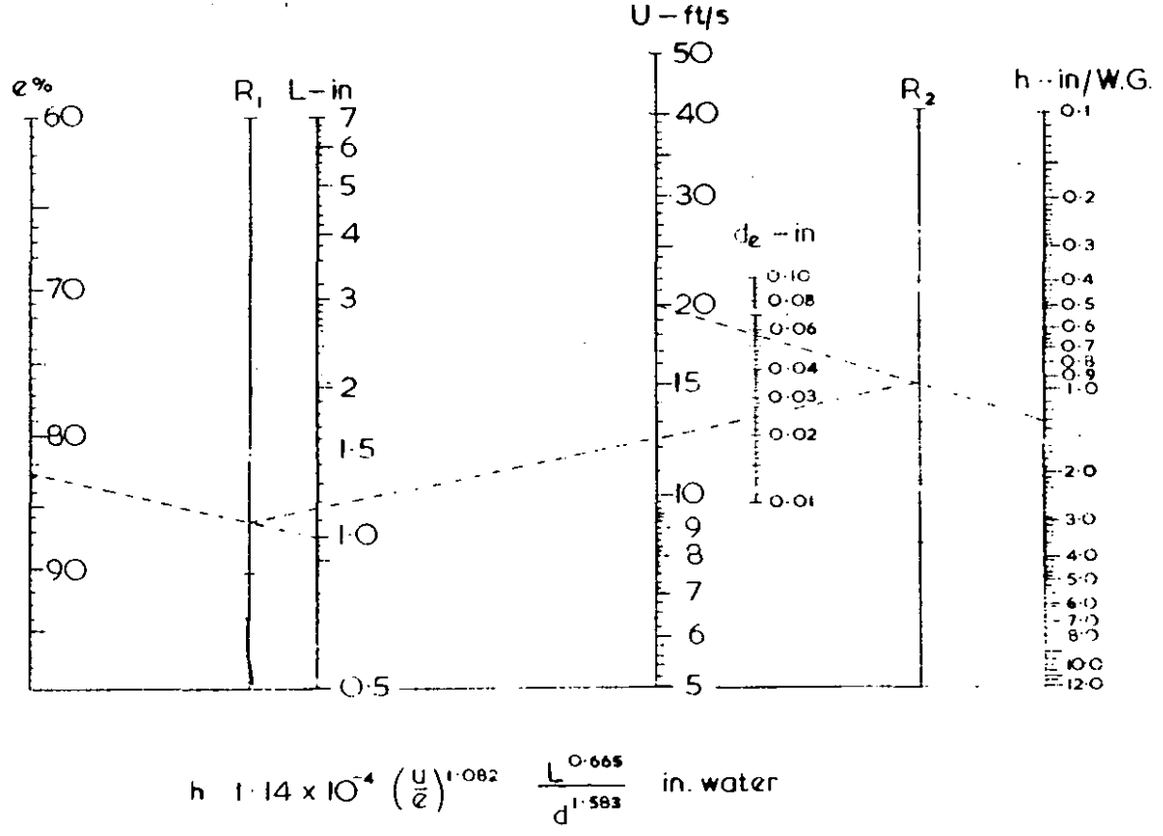

$$h \quad 1{\cdot}14 \times 10^{-4} \left(\frac{u}{e}\right)^{1{\cdot}082} \frac{L^{0{\cdot}665}}{d^{1{\cdot}583}} \quad \text{in. water}$$

FIG. 7 NOMOGRAM FOR THE PRESSURE DROP ACROSS CRIMPED-RIBBON FLAME ARRESTERS

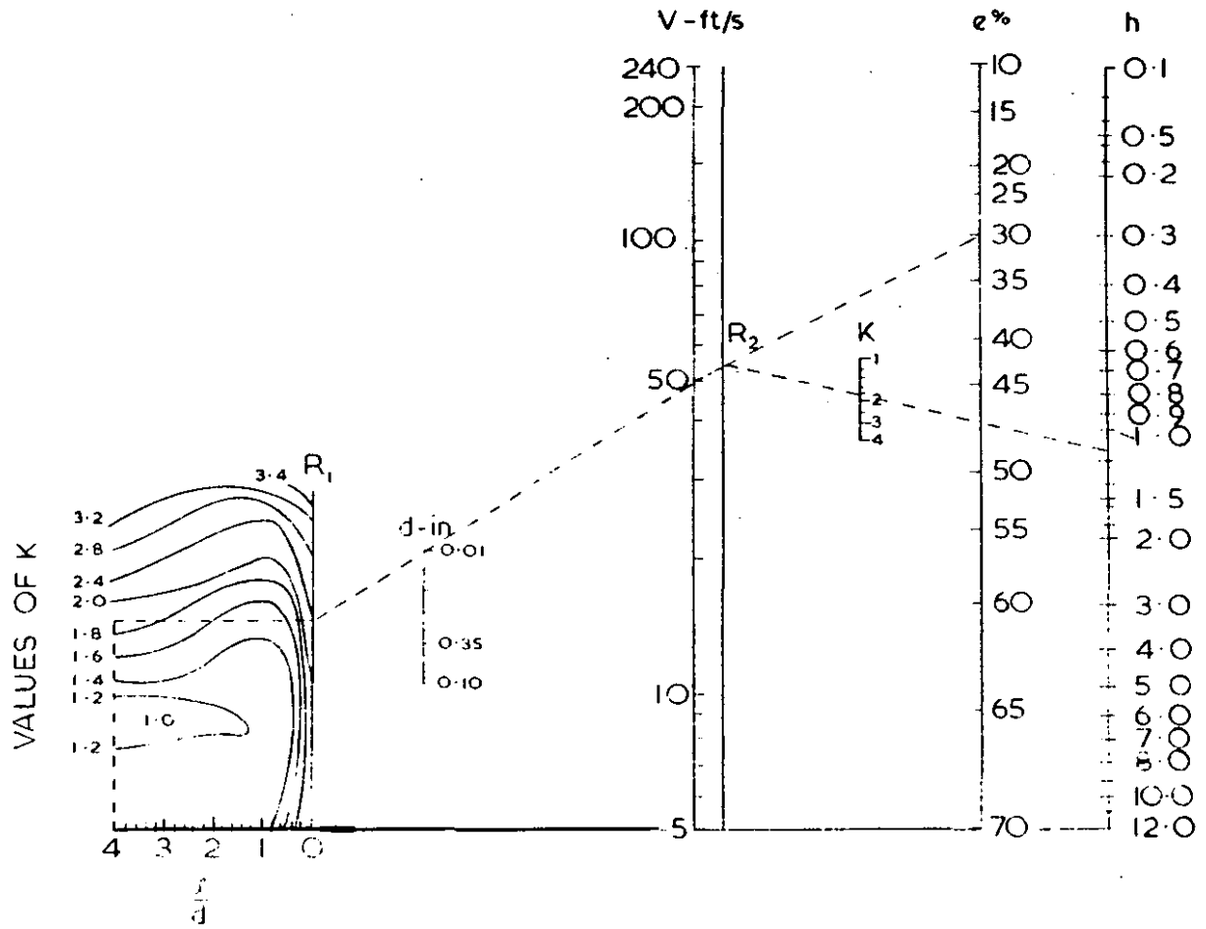

FIG. 8 NOMOGRAM FOR THE PRESSURE DROP ACROSS PERFORATED PLATE FLAME ARRESTERS